WORLD JOURNAL OF PHARMACEUTICAL RESEARCH
SJIF Impact Factor 7.523
Volume 5, Issue 12, 1538-1565. Research Article ISSN 2277– 7105

EFFECT OF TAMOXIFEN ON PRENATAL AND POSTNATAL DEVELOPMENT OF KIDNEY IN ALBINO RAT'S OFFSPRING

Eman Badawi Elshal*[1], Zakia Ibrahim Abdelhameid[1] and Hassan Fathy[2]

[1]Anatomy Departments, Faculty of Medicine for Girls-, Al-Azhar University.

[2]Histology Departments, Faculty of Medicine, Al-Azhar University.

Article Received on
20 October 2016,

Revised on 10 Nov. 2016,
Accepted on 30 Nov. 2016

DOI: 10.20959/wjpr201612-9572

***Corresponding Author**
Eman Badawi Elshal
Anatomy Departments,
Faculty of Medicine for
Girls-, Al-Azhar University.

ABSTRACT

Breast cancer is a major health problem worldwide and is the second cancer leading death especially for women. Tamoxifen (TAM), a non-steroidal antiestrogen, used as a chemotherapeutic and chemopreventive agent for breast cancer. The aim of this study was to investigate the teratogenic effects of tamoxifen on the developing kidney of the offspring of the Sprague Dawley rat at the 20th day of gestation (GD20) and at the postnatal 7th day (PND7) after delivery. **Materials and methods:** sixty adult Sprague Dawley 20 male and 40 female albino rats were used in this experiment. Forty pregnant albino rats were divided into two equal groups: **group I** (control) and **group II** (treated). Each group was subdivided into 2 subgroups. Each subgroup was consisted of (10 pregnant rats). In **Group IB (GD20)**, tamoxifen was administered orally at a dose of 0.36 mg /day through orogastric tube for 19 days from the 1st day (GD1) to the 19th day (GD20) of gestation. In **group IIB (PND7)** treated group: Tamoxifen was administered daily at a dose of 0.36 mg tamoxifen orally through orogastric tube for 28 days from the (GD1) to (PND7) after delivery. At the end of the experiment the male offspring (GD20) and (PND7) were sacrificed. The kidney of both control and treated groups were dissected and prepared for histological examination by light and electron microscopy. The number of fetuses and their weights were recorded. **Results:** There was a significant decrease in the overall body weight in both TAM treated groups (GD20 and PND7) when compared with the control group. TAM treatment in (PND7) induced significant increase in serum levels of kidney biomarkers, creatinine, urea, and uric acid. Microscopic examination of the kidnies of both (GD20) and (PND7) treated groups, revealed small atrophied glomeruli. Some of them appeared shrunken with dilated capsular space. The proximal and distal tubules were swollen

with loss of some of their nuclei. Many areas of focal necrosis were seen with tubular degeneration, partial loss of the luminal brush border. Ultrastructural results in (PND7) treated group, the glomeruli appeared immature. The renal corpuscles showed the endothelial cells was detached at certain points some of their fenestrations were obliterated, focal fusion of podocytes foot processes and irregular thickening of glomerular basement membranes. **Conclusion:** Tamoxifen induced developmental structural changess in the kidney during pregnancy and breast feeding. Therefore, tamoxifen should not be prescribed for either pregnant or lactating mothers.

KEYWORDS: Kidney, tamoxifen, prenatal, postnatal development, rat.

INTRODUCTION

Breast cancer remains the most common malignancy in women all over the world. Estrogen levels appear to be associated with an increased risk for the development of breast cancer **((Lo and Vogel 2004).** Tamoxifen (TAM) is a drug that has been in worldwide use for the treatment of anti estrogen receptor (ER) positive breast cancer cases for over 30 years; it has been used in both the metastatic and adjuvant setting **(Lazzeroni et al.,2012).** It can be used in both pre- and postmenopausal women who are at increased risk of breast cancer **(Fisher et al.,2005)**. Tamoxifen, a triphenylethylene derivative, is the only proven oral agent for the treatment and prevention of all stages of hormone dependent breast cancer (**Desai et al., 2002; Colleoni et al., 2006).** In 1998 the National Surgical Adjuvant Breast and Bowel Project (NSABP) demonstrated that Nolvadex treatment reduced the incidence of both invasive and non-invasive breast cancer in population at high risk for disease **(Tan- Chiu et al., 2003).** With the widespread use of tamoxifen, attention has been focused on its adverse effects, particularly toxicity to various organs **(Dray et al., 2000).** The reported cases of non-alcoholic steatohepatitis with cirrhosis in tamoxifen-induced fatty liver has been observed in more than 30% of breast cancer patients who received adjuvant tamoxifen treatment (**Elefsiniotis et al., 2004**). TAM-induced hepatorenal toxicity was also previously reported **(Parvez et al., 2006)**. Recent evidence suggested that the generation of reactive oxygen species (ROS) and oxidative stress may also play a role in the TAM induced organ toxicity **(Jin et al., 2005; Dragan et al., 1996).**

In addition, antineoplastic agents or adjuvant treatments including TAM were suggested to directly cause impairment of the renal functions **(Kintzel and Dorr 1995).**

Tamoxifen therapy was not recommended during pregnancy, mainly because it may cause fetal abnormalities **(Cullins et al., 1994)**. For example, animal studies have linked a maternal exposure to tamoxifen during pregnancy with abnormalities in the reproductive tracts of the offspring **(Diwan et al., 1994)**, some of these abnormalities were similar to those caused by fetal exposure to synthetic estrogen diethylstilbestrol and others were specific to tamoxifen **(Sato et al., 1996)**. Estrogenic manipulations during fetal life through pregnant mothers alter breast cancer risk among daughters.

The aim of this study is to investigate the teratogenic effects of tamoxifen on the kidney of the offspring at a prenatal and early postnatal period; 20th day of gestation (GD20) and the postnatal 7th day (PND7) respectively.

MATERIAL AND METHODS

Drugs: Nolvadex (tamoxifen citrate 40 mg) was purchased from AstraZeneca (Egypt). In this study the equivalent to the human therapeutic dose for an adult rat weighing about 200 g was calculated by using the formula of **Paget and Barnes (1964)** to be 20x18/1000 = 0.36 mg/rat/day. Milling of the tablets in the form of powder was done. For each pregnant rat a daily dose 0.36 mg was weighted, dissolved in 1 ml of distilled water and administrated in to the pregnant rats.

Experimental Animals

Animals

Sixty adult Sprague Dawley 20 male and 40 female albino rats were used in this experiment, with average weight 200-250 gm. The animals were purchased from the Plasma Purification Center, Helwan, Cairo, Egypt. Animals were caged separately, males in cages and females in others. All rats were housed in a quite non-stressful environment for one week before beginning of the present study. They were offered normal rat chows and water *ad libitum* during the experimental period.

Each male was kept overnight with two female in a separate cage. The female were examined for vaginal plugs to be considered the first day of pregnancy and was designated as gestation day 0 (GD0) with subsequent days of gestation were numbered **(Butkevich et al., 2003)**. The pregnant rats were kept in a separate cage for continuation of the experiment. The offsprings were kept with their mothers for feeding. Forty pregnant rats were divided into two groups,

the control and the treated groups. Each group was subdivided into 2 subgroups. Each subgroup was consisted of (10 pregnant rats).

Group I was the (prenatal) GD20 at 20th day of gestation

This group was subdivided into 2 subgroups

- **Group I A (GD20) control group:** 1 ml distilled water was administered to animals in this group orally from GD 1- 19th day of gestation. The mothers were anesthetized and the embryos were extracted. Pregnant females gave about 50 embryos, 24 of them were males.
- **Group IB (GD20) treated group:** Tamoxifen was administered for animals in this experimental group at a daily dose of 0.36 mg tamoxifen orally after dissolving in 1 ml of distilled water through orogastric tube from GD 1- 19th day of gestation. The mothers were anesthetized and the embryos were extracted the females gave about 35 embryos 15 of them were males, which were examined for any morphological deformities.

Group II was the postnatal day (PND7) at 7th day after birth.

This group was subdivided into 2 subgroup

- **Group IIA (PND7) control group:** it was administered oral doses of 1 ml of distilled water orally through orogastric tube from GD 1 to 7th day after delivery. The mothers' gave about 50 embryos 25 of them were males, which were examined.
- **Group IIB (PND7)treated group:** it was administered a daily dose 0.36 mg tamoxifen orally through orogastric tube from GD 1 to 7th day after delivery. The females delivered about 30 embryos 18 of them were males.

At the end of the experiment the male offspring at 20th day of gestation and the newborn stage (PND7) were sacrificed. The kidney of both control and treated groups were dissected and prepared for histological study.

Sample collection

At the end of experiment there was difficulty to collect blood samples from (GD20) groups. So, the blood samples were collected from the (PND7) at 7th day after delivery by cardiac puncture and animals were decapitated. The samples were centrifuged at 3000 rpm for 15 min to separate the serum. The serum was then frozen at –20°C for the subsequent estimation of biochemical parameters.

Biochemical parameters to test the levels of renal function markers included serum creatinine, urea, uric acid, albumen and total protein were determined using the appropriate commercially available kits (Bio-Diagnostic, Dokki, Giza, Egypt).

Histological Preparation for Light Microscope Investigation

The right kidneys were fixed in 10% neutral formalin for 48 hours. Tissues were dehydrated in ascending concentrations of alcohol, cleared in xylene, and embedded in paraffin. Five micrometer-thick sections were prepared and stained with Haematoxylin and Eosin for histological examination. Polysaccharides accumulations were investigated through detection of the periodic acid Schiff's (PAS) reagent and collagen fibers were stained by using Mallory's trichrome staining method **(Bancroft and Gamble, 2013).**

II-Transmission electron microscope study

The left kidney from each animal was placed on a sheet of dental wax in a drop of primary fixative and its cortex was cut into minute pieces. The specimens from all groups were fixed in 2.5% glutaraldehyde and post fixed in 1% osmium tetroxide, dehydrated and embedded in epoxy resin. One µm sections (semithin sections) were preliminary obtained and stained with toluidine blue. Ultrathin sections were cut and double stained with uranyle acetate and lead citrate, then examined by transmission electron microscope (**Glauert and Lewis, 1998)**.

Statistical study: was done for the following: i) body weight estimation, ii) serum kidney biochemical markers included creatinine, urea, and uric acid, albumen and total protein. The collected data was subjected to statistical analysis using SPSS statistics software for Windows, version 17.0. (Chicago: SPSS. Inc.2008). Descriptive statistics: Data were presented as mean± standard error of the mean (SEMD). Analytical statistics: used for comparison between groups and this was performed using *Student's t-test*. Significance level: was set at $P < 0.05$ for all comparisons. So, Values of $P < 0.05$ indicated significant, $p < 0.01$ and $p < 0.001$ was highly significant difference between control and treated groups. The results were presented in tables and histograms (Rosner, 1990).

RESULTS

Body weight study

At the end of the experimental study, the body weight for the offspring revealed highly statistically significant reduction of the treated subgroups (group IB and group IIB) in

comparison to the control subgroups (group IA and group IIA), as shown in table (1) and histogram (1).

Table 1: Body weight measurements in the control and tamoxifen treated groups.

Weight	Control	Treated
(GD20)	4.933 ± 0.431, n=6	3.667 ± 0.3333, n=6, *
(PND7)	14.17 ± 0.48, n=6	10.00 ± 0.58, n=6, ***

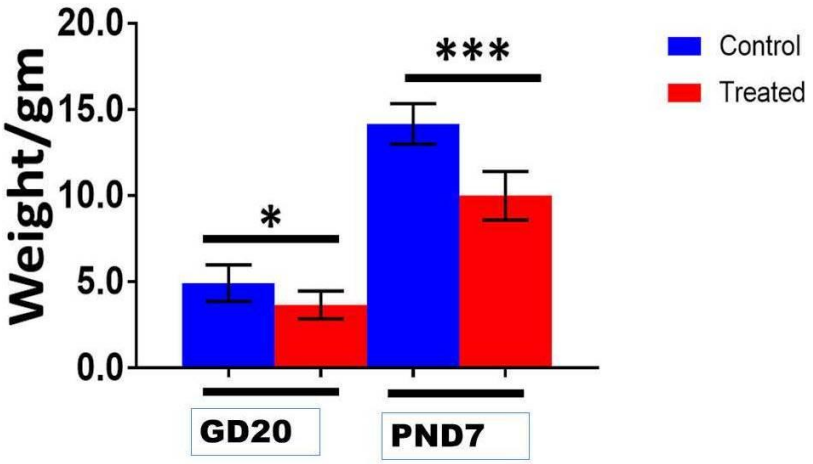

Histogram 1: Mean values of the body weight of the studied groups.

Kidney function test

The biochemical analysis for the kidney function test, in group IIB (PND7) treated with TAM for 28 days showed that significant increase ($P < 0.001$) in the nitrogenous end products; serum creatinine, urea and uric acid, which reflect the efficacy of kidney function. While, there were significant ($P < 0.001$) decrease in the serum level of albumen and total proteins as compared to the control one as shown in table (2) and histogram (2, A,B,C,D,E).

Table 2: Renal function markers of (PND7) rats.

Kidney function test	Control	TAM treated
Blood Urea	4.42 ± 0.521, n=10	9.31 ± 1.705, n=10, *
Serum Creatinine	0.879 ± 0.1852, n=10	1.64 ± 0.02449, n=10, ***
Uric Acid	174.9 ± 11.47, n=10	267.8 ± 28.09, n=10, **
Albumin	169.4 ± 21.39, n=10	9.34 ± 0.2982, n=10, ***
Total proteins	49.8 ± 0.611, n=10	30.6 ± 0.1633, n=10, ***

Table 2: Biochemical analysis of the kidney function tests in the TAM treated animals as compared to the control.

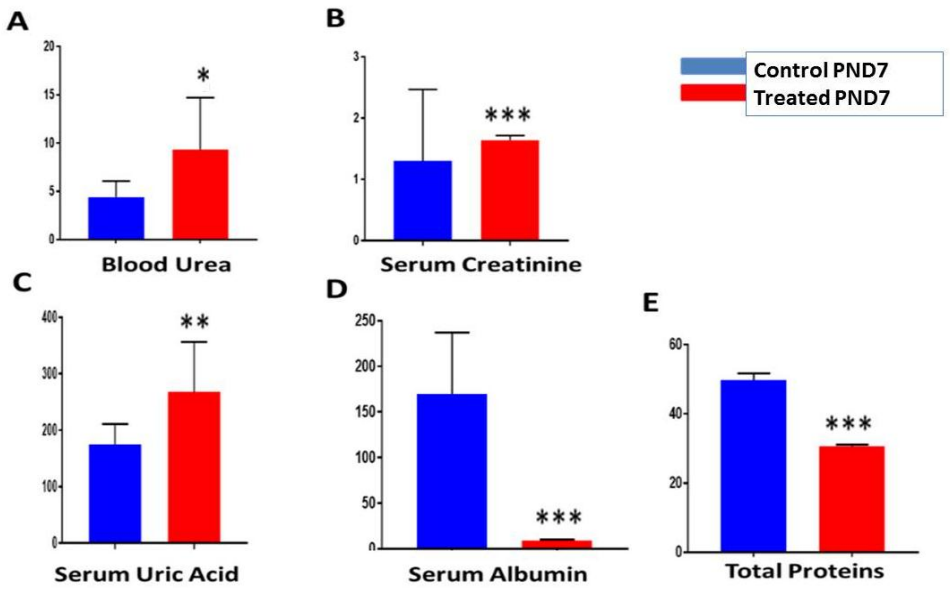

Histogram (2): Mean values of the kidney function and the statistical differences are indicated by **P < 0.05 is significant, **P < 0.01, ***P < 0.001 is highly significant* when compared with control animals.

Light microscope examination

Group I A (GD20) control group

The examination of H&E stained sections of the **(GD20)** control kidney of albino rat, showed that the kidney was surrounded by fibrous connective tissue capsule. The kidney was differentiated into outer cortex and inner medulla. The renal cortex was characterized by the presence of two cortical zones, the subcapsular zone contained immature forms of the renal corpuscles in developmental stages; the juxtamedullary zone contained mature renal corpuscles, which appeared larger than the subcapsular zone. The medullary rays were extending through the cortex to the medulla and divided the kidney into renal lobules surrounding each medullary ray (Fig. 1A). The malpighian renal corpuscles were formed of Bowman's capsules surrounding tuft of blood capillaries. The Bowman's capsules was formed of outer parietal layer and inner visceral layer of podocytes which merged the glomerular tuft of capillaries. Each blood capillary within the capillary tuft was formed of glomerular basement membrane (GBM) and lined by simple squamous endothelium. Some proximal convoluted tubules (PCTs) was formed of a single layer of columnar cells with rounded basal nuclei and acidophilic granular cytoplasm, its luminal border (free border) had fine brush border. Distal convoluted tubules (DCTs) showed a dilated lumen with a smooth free border. Their cells were cubical with rounded deeply stained nuclei and less acidophilic and nongranular cytoplasm (Fig.1B).

Masson's Trichrome stained sections showed that normal distribution of collagen fibers around and in the renal corpuscles and tubules (Fig.1C).

PAS stained sections showed that PAS positive reaction in the brush borders of the tubules and basement membrane of renal tubules and glomerular capillaries (Fig. 1D).

Group IB (GD20) treated group

The examination of H&E stained sections **(GD20)** treated kidney of rat showed that the kidney was surrounded by thin irregular fibrous connective tissue capsule and divided into outer cortex and inner medulla. The medullary rays could not be recognized. The renal cortex had crowded immature renal glomeruli in the subcapsular zone. However, the deeper cortex had some atrophied glomeruli (Fig.2A). By higher magnification some of the glomeruli appeared shrunken with disrupted reduced glomerular tuft of capillaries and dilated capsular space. Other glomeruli appeared destructed with darkly stained nuclei and obliterated Bowman's space, even they appeared merging with the surrounding tissue. General tubular configuration was lost with some vacuolar spaces present between the kidney tissues. The proximal and distal tubules were swollen with loss of some of their nuclei. Some of the proximal and distal tubules were lined by small deeply stained pyknotic nuclei and others with apoptotic cells (Fig.2B).

Masson's Trichrome stained sections showed that increase in the amount of collagen fibers in between the renal tubules, around and within the renal corpuscles. Foci of interstitial fibrosis were also noticed as compared with control (Fig. 2C).

PAS stained sections showed decrease in PAS positive reaction in the brush borders of most of the tubules and basement membrane of renal tubules and glomerular capillaries when compared with control (Fig. 2D).

Group IIA (PND7) control group

The examination of H&E stained transverse sections of the **PND7** control kidney of albino rat, showed that the kidney was covered by capsule and differentiated into outer cortex and inner medulla. The renal corpuscles in the cortex appeared uniform in appearance with disappearance of most of the immature forms. The medullary rays were extending from the cortex to the medulla (Fig.3A). By higher magnification the renal corpuscles at the subcapsular zone appeared spherical in shape and the Bowman's capsules appeared with

distinct Bowman's space. The Bowman's capsule was formed of parietal and visceral layers. The parietal layer of Bowman capsule was formed of flat cells and the visceral layer was closely applied to the glomerular capillaries. The PCT cells showed vesicular rounded basal nuclei with acidophilic granular cytoplasm and characteristically narrow lumen. The DCTs were lined by more cuboidal cells with less acidophilic cytoplasm and characteristically wide lumen (Fig. 3B).

Masson's Trichrome stained sections showed that the normal distribution of collagen fibers around and in the renal corpuscles and tubules (Fig.3C).

PAS stained sections showed that PAS positive reaction in the brush borders of the tubules and basement membrane of renal tubules and glomerular capillaries (Fig.3D).

Group IIB (PND7) treated group

The examination of H&E stained sections of the **PND7** treated kidney of albino rat, showed that the kidney was covered by capsule and differentiated into outer cortex and inner medulla (Fig.4A). There were degenerative changes in both glomeruli and tubules. There was atrophy of glomerular capillaries, deformity; the parietal layer of Bowman's capsules was thick while the visceral layer was hardly seen. The glomerular tuft of capillaries was irregular with disturbed capsular space. There were degeneration of tubular epithelial lining and inter tubular acidophilic tissue remnants (Fig.4B). Both PCTs and DCT were lined by simple cubical epithelium. Some of these cells were degenerated and showed necrosis with scattered apoptotic, karyolitic nuclei (Fig.4B).

Masson's Trichrome stained sections showed that increase in the amount of collagen fibers in the renal tubules, around and within the renal corpuscles. Foci of interstitial fibrosis were also noticed as compared to the control. There was an increase in the amount of collagen fibers in the renal capsule (inset on the right) of (Fig.4C).

PAS stained sections showed that decreased in PAS positive reaction in the brush borders of the tubules and basement membrane of renal tubules and glomerular capillaries when compared with control (Fig.4D).

Semithin sections of the PND7control kidney albino rat, showed that the mature renal corpuscle. Each renal corpuscle was formed of a glomerular tuft of capillaries surrounded by Bowman's capsule, the Bowman's space was between the two layers. The parietal layer was

lined with simple squamous epithelium, while the visceral layer formed of podocytes investing and merging with the glomerular capillaries. Some capillaries were identified by the endothelial cells and red blood cells within the lumen. Intra glomerular mesangial cells were identified by their densely stained nuclei and were surrounded by a deeply stained matrix between the glomerular capillaries (Fig.5). The proximal convoluted tubules and distal convoluted tubules were also seen (Fig.5).

Semithin sections of the PND7 treated kidney albino rat, showed that there were delayed in development of the renal corpuscles. The comma shaped bodies were formed of double wall of simple columnar epithelium and mitotic figures. The Bowman's space was hardly seen and was surrounded by cells of parietal layer. The renal vesicles appeared with central lumen and radially oriented tall columnar cells with basal oval nuclei and mitotic figures. The PCTs was disrupted and DCTs also its cells had mitotic figures (Fig.6).

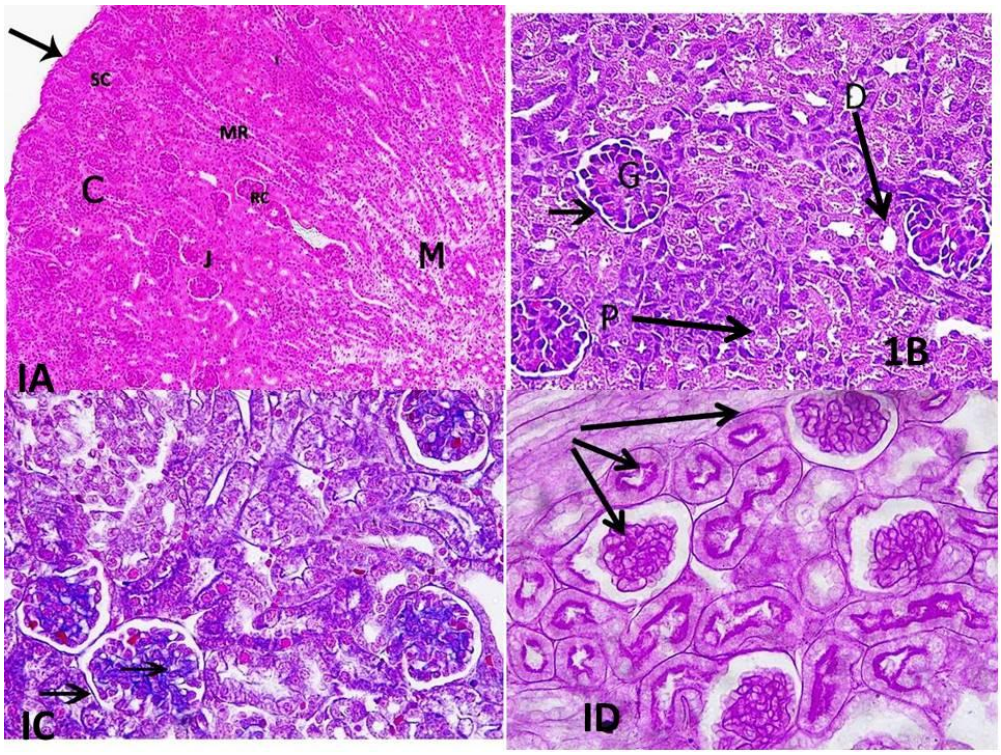

Figure 1A: photomicrographs of the kidney **group IA (GD20) control group, showing** the kidney was surrounded by connective tissue capsule (C) and differentiated into outer cortex (C) and inner medulla (M). The renal cortex has two cortical zones. The subcapsular zone (SC) contained immature forms of the renal developmental stages and the juxtamedullary zone (J) contained mature renal corpuscles. The medullary rays(MR) appeared radiating from the cortex through the medulla. **H &E X100.**

Figure 1B: photomicrographs of the renal cortex **group IA (GD20) control group, showing** the glomeruli (G) have Bowman's capsules with its outer parietal layer (arrow). The proximal convoluted tubules (P) was formed of a single layer of columnar cells with rounded basal nuclei and acidophilic granular cytoplasm, its luminal border (free border) had fine brush border. Distal convoluted tubules (D) showed a dilated lumen with a smooth free border. **H & E X400.**

Figure 1C: photomicrographs of the renal cortex **group IA (GD20) control group,** showing normal distribution of collagen fibers around and in the renal corpuscles and tubules (arrow). **Masson's Trichrome x400 Figure 1D:** photomicrographs of the renal cortex **group IA (GD20) control group,** showing PAS positive reaction in the brush borders of the PCT and basement membrane of renal tubules and glomerular capillaries (arrow). **PAS x400.**

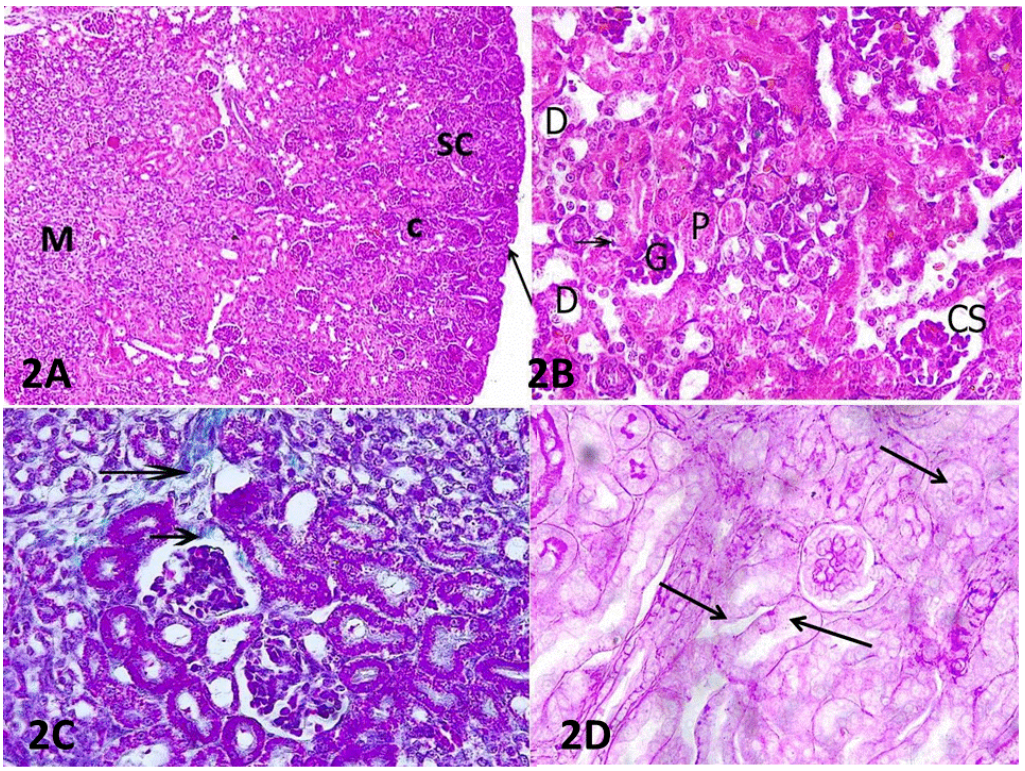

Figure 2A: photomicrographs of the kidney **group IB (GD20) treated group, showing** irregular fibrous connective tissue capsule (arrow) and divided into outer cortex (C) and inner medulla (M). There was disruption of the medullary rays. The renal cortex has crowded immature renal glomeruli in the subcapsular zone (SC). **H &E X100.**

Figure 2B: photomicrographs of the renal cortex **group IB (GD20) treated group, showing** the deeper cortex has small atrophied glomeruli (G). Some of them appears shrunken with

disrupted glomerular tuft of capillaries and dilated capsular space (CS). The proximal (P) and distal tubules (D) are swollen with many areas of focal necrosis, apoptotic cells (arrow) and have vaculated cytoplasm and pyknotic nuclei. **H &E X400.**

Figure 2C: photomicrographs of the renal cortex **group IB (GD20) treated group, showing** that increase in the amount of collagen fibers in the renal tubules, around and within the renal corpuscles. Foci of interstitial fibrosis are also seen (arrow). **Masson's Trichrome x400**.

Figure 2D: photomicrographs of the renal cortex **group IB (GD20) treated group, showing** decrease in PAS positive reaction in the brush borders of the PCT and basement membrane of renal tubules and glomerular capillaries. **PAS x400.**

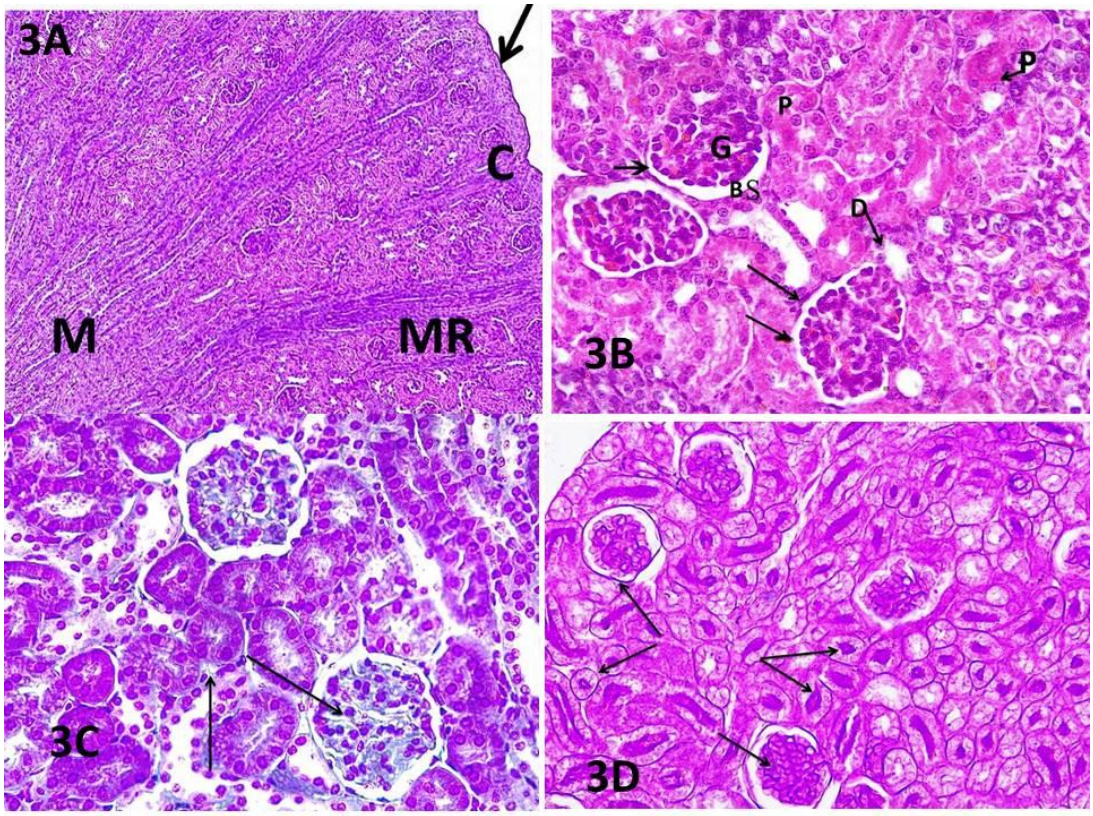

Figure 3A: photomicrographs of the kidney **of group IIA PND7 control albino rat** showing, the kidney was covered by capsule (arrow) and differentiated into outer cortex (**C**) and inner medulla (**M**). The medullary rays were extending from the cortex to the medulla **(MR)**. **H &E X100.**

Figure 3B: photomicrographs of the renal cortex **of group IIA PND7control albino rat** showing, the glomeruli (G) appear spherical in shape and the Bowman's capsules appear with distinct Bowman's space (BS). The Bowman's capsule is formed of parietal (arrow) and

visceral layers. The PCT cells (P) showed vesicular rounded basal nuclei with acidophilic granular cytoplasm and characteristically narrow lumen. The DCTs (D) are lined by more cuboidal cells with characteristically wide lumen. **H &E X400**

Figure 3C: photomicrographs of the renal cortex **of group IIA PND7 control albino rat** showing, normal distribution of collagen fibers around and in the renal corpuscles and tubules **Masson's Trichrome x400**

Figure 3D: photomicrographs of the renal cortex **of group IIA PND7 control albino rat** showing, PAS positive reaction in the brush borders and basement membrane of renal tubules and glomerular capillaries. **PAS x400.**

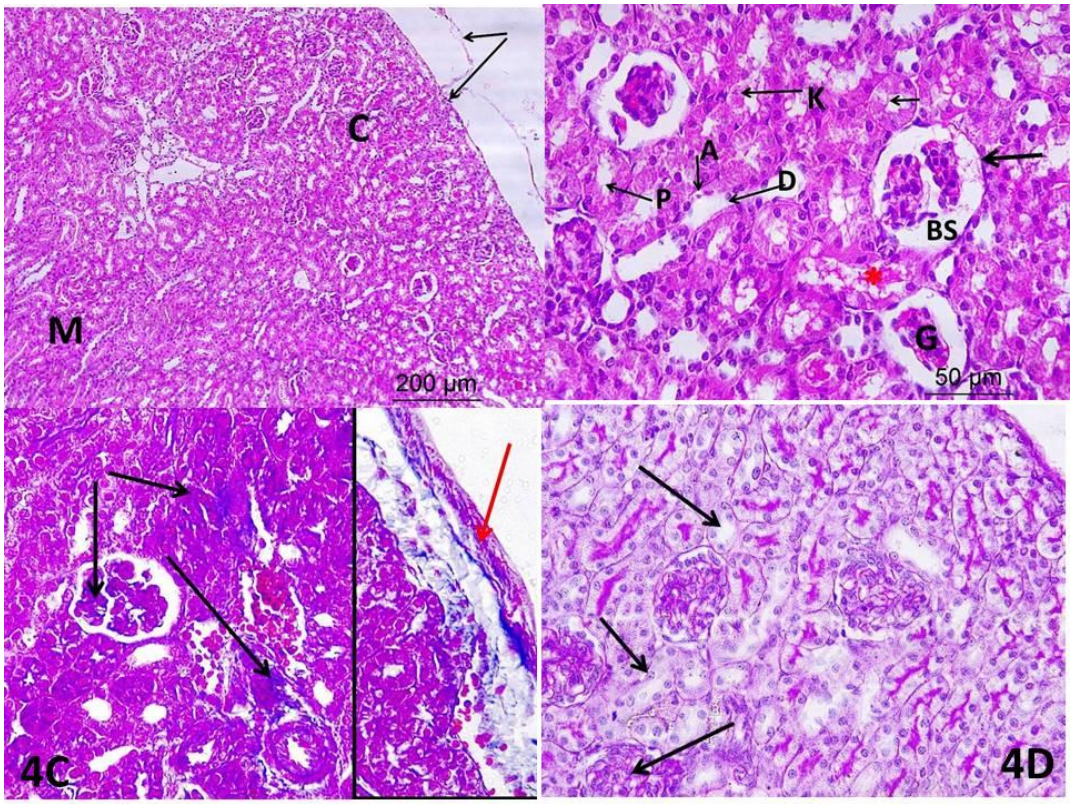

Figure 4A: photomicrographs of the kidney **of group IIB (PND7) treated albino rat** the kidney was covered by detached capsule (arrow) and differentiated into outer cortex (**C**) and inner medulla (**M**). The medullary rays cannot be seen. **H &E X100.**

Figure 4B: photomicrographs of the renal cortex **of group IIB (PND7) treated albino rat** showing there is atrophy of glomeruli (G) with dilated capsular space (CS), the parietal layer of Bowman's capsules is thick (arrow). There are degeneration of tubular epithelial lining and

inter tubular acidophilic tissue remnants (red asterisk). Some cells of both PCTs (P) and DCT (D) shows degeneration with scattered apoptotic (A), karyolitic (K) nuclei. **H &E X400.**

Figure 4C: photomicrographs of the renal cortex **of group IIB (PND7) treated albino rat** showing: increase in the amount of collagen fibers in the renal tubules, around and within the renal corpuscles (arrow). Foci of interstitial fibrosis (asterisk) were also noticed as compared with control. Notice also the increase in the amount of collagen fibers in the renal capsule (**inset on the right**) (red arrow). **Masson's Trichrome x400.**

Figure 4D: photomicrographs of the renal cortex **of group IIB (PND7) treated albino rat** showing: PAS positive reaction decreases in the brush borders and basement membrane of renal tubules and glomerular capillaries **PAS x400.**

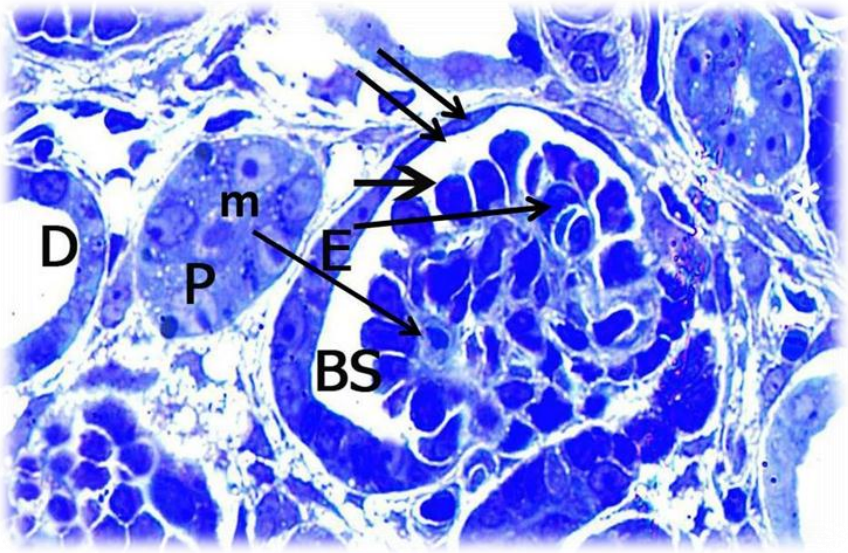

Figure 5: photomicrographs of a **semithin section of** the renal cortex **of group IIA PND7 control albino rat** showing oval maturing glomeruli containing numerous capillary loops and their endothelial cells (E). The Bowman's space is seen (BS). The parietal layer is formed of flattened cells (2 arrows) and the cells of the visceral layer are seen surrounding the capillaries loops (arrow). Mesangial cells are also found (m). PCTs (P) and DCTs (D) convoluted tubules are also seen. **TB × 1000.**

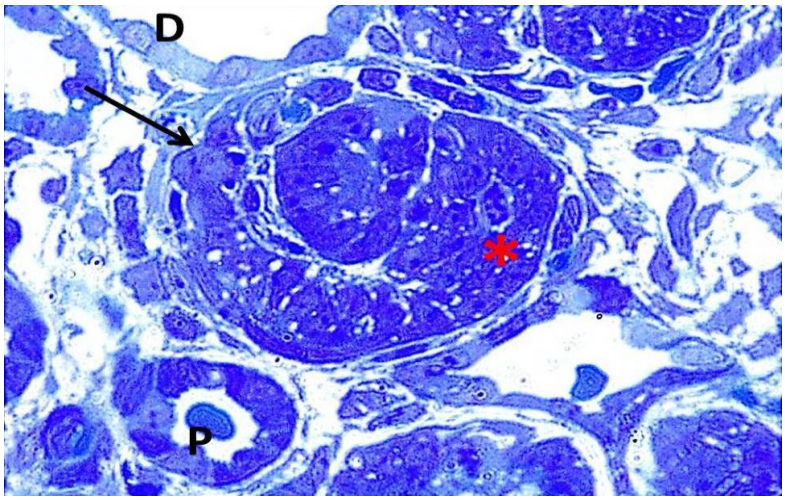

Figure 6: photomicrographs of a **semithin sections of** the renal cortex **of group IIB (PND7) treated albino rat** showing the renal vesicles appears with central lumen and radially oriented tall columnar cells with basal oval nuclei and mitotic figures(asterisk). The Bowman's space is hardly seen (arrow), the PCTs (P) is disrupted and DCTs also seen. **TB × 1000.**

Electron microscope examination

Group IIA PND7

Electron microscopic examination of the renal cortex of **group IIA PND7 control albino rat** revealed normal appearance of the glomeruli, where capillary loops showed thin layer of the fenestrated endothelial cells while the parietal layer contains large flat cells in close contact with glomerular basement membrane called podocytes. Podocytes nuclei were irregular and their primary process gave rise to secondary foot processes which rested on the glomerular basement membrane (Figure 7, 8). The glomerular basement membrane separated the podocytes and the capillary endothelium. The thickness of the basement membrane was nearly uniform. The three components of the glomerular filter were seen; the fenestrated capillary endothelium which was closely applied to the luminal surface, on the opposite side the podocytes secondary foot processes were seen and the glomerular basement membrane could be seen in between two previously mentioned layers (Figure 9). The proximal convoluted tubule was characterized by large cuboidal cells had prominent brush border of dense microvilli. The cytoplasm immediately beneath the microvilli contained many pinocytic vesicles and few lysosomes. The nucleus was rounded and basally located. There were numerous scattered mitochondria arranged in longitudinal axis of the cell and in between basal membrane (Figure 10). The distal convoluted tubule had ultrastructure features in common with the PCT especially the large number of mitochondria. The most striking

difference was the DCT had few irregular microvilli along the apical side of the cells. The DCT had less cytoplasm than those of the PCT and their nuclei were occupying most of the cell. The nuclei appeared oval euchromatic nuclei and close to the luminal surface (Figure11).

Group IIB PND7

The ultrastructure examination of the renal cortex of **group IIB PND7 tamoxifen treated albino rat**, showed the renal corpuscle contained blood capillaries which contain the red blood cells (RBCs) and lined by fenestrated endothelial cells. The endothelial cells were detached at certain points from the basement membrane (Figure 12). By higher magnifications enabled visualization of fenestration of the glomerular basement membrane which was obliterated at certain points. The secondary foot processes were fused at certain points of the Bowman's capsule, the persistence of the membrane ou tpocketings of the loop pattern revealed under developed podocytes foot processes (Figure 13,14). The PCTs, cells appeared with resting on distorted basement membrane, small nuclei, the apical microvilli appear less dense and disrupted more frequent enlarged cytoplasmic vacuoles and with enlarged lysosomes. The mitochondria appeared rounded and swollen (Figure 15). The distal convoluted tubule appeared smaller with less developed apical microvilli and some cells were completely devoid of the apical microvilli, abnormal detached basement membrane, fragmented abnormal mitochondria and abnormal tight junctions in between epithelial cells (Figure 16).

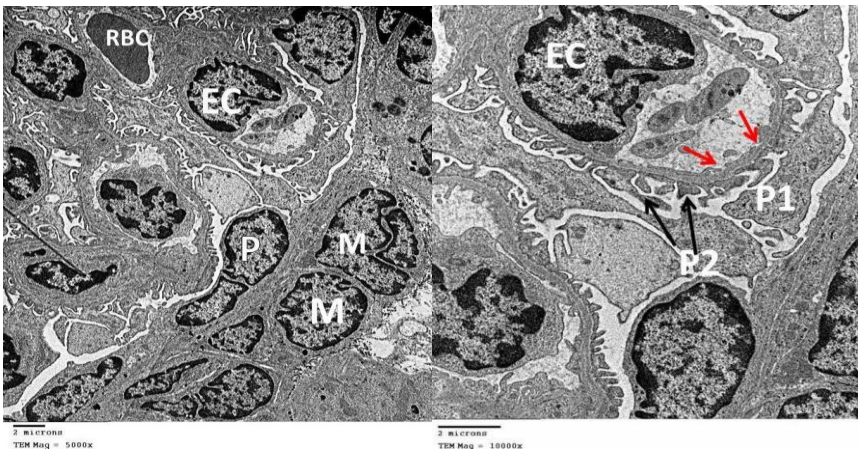

Figure 7: photomicrographs of **ultrathin section of** the renal corpuscle **of group IIA PND7 control albino rat** showing: the blood capillary is lined with endothelial cells (EC), red blood cell (RBC) inside it. The podocytes (P) and mesangial cells (M) are surrounding the glomerular blood capillary. **TEM x 5000.**

Figure 8: photomicrographs of a higher magnification of the previous figure **of group IIA PND7 control albino rat** showing: The glomerular filtration membrane is formed of a double layer membrane lined with endothelial cells (EC) with endothelial fenestrations (red arrows) in between them. The podocytes (P) appear with well- developed primary (P1) and foot processes (P2). **TEM x 10000.**

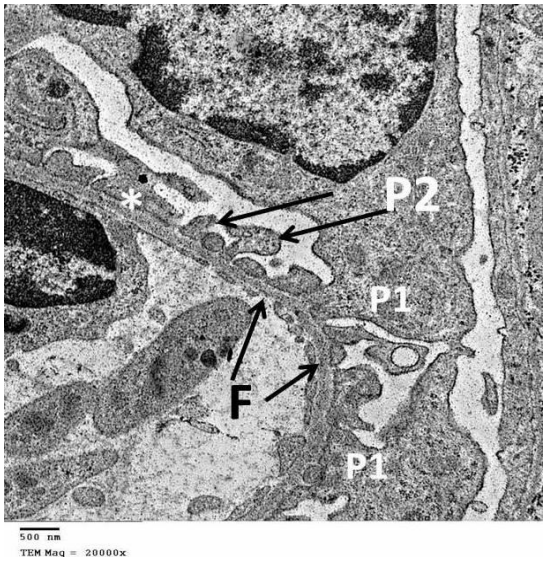

Figure 9: photomicrographs of a higher magnification of the previous figure **of group IIA PND7 control albino rat** showing: part of capillary loop with fenestration of endothelial cells (F), glomerular basement membrane (asterisk), and well-developed primary foot processes (P1) and secondary foot processes (P2). **TEM x 20000.**

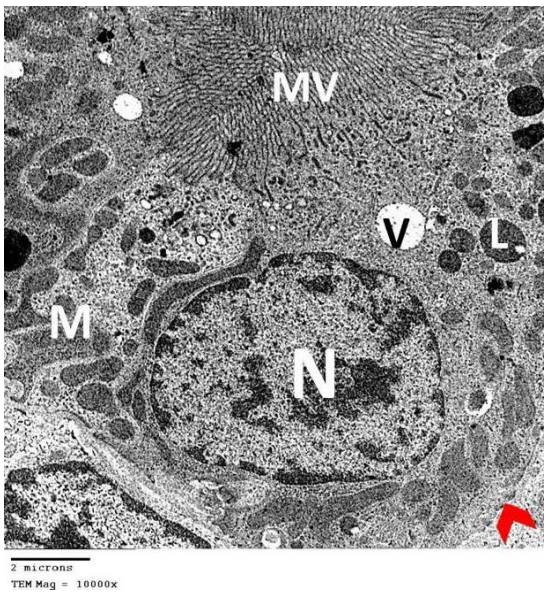

Figure 10: photomicrographs of **ultrathin section of** the PCT **of group IIA PND7 control albino rat** showing the PCT is lined with epithelial cells resting on a basement membrane

(arrow head) with euchromatic nuclei (N), well developed luminal microvilli (MV), pinocytic vesicles (V) small round lysosomes (L) and elongated mitochondria (M). **TEM x 10000.**

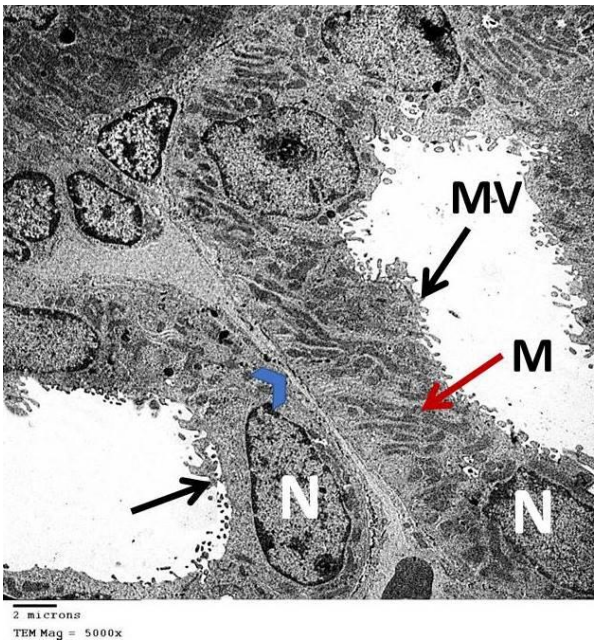

Figure 11: photomicrographs of **ultrathin section of** the DCT **of group IIA PND7 control albino rat** showing the cells of distal renal tubules appeared resting on well-developed basement membrane (blue arrow head) with oval euchromatic nuclei (N), with microvilli (MV) along their apical border, elongated and highly abundant mitochondria (M). **TEM x 5000.**

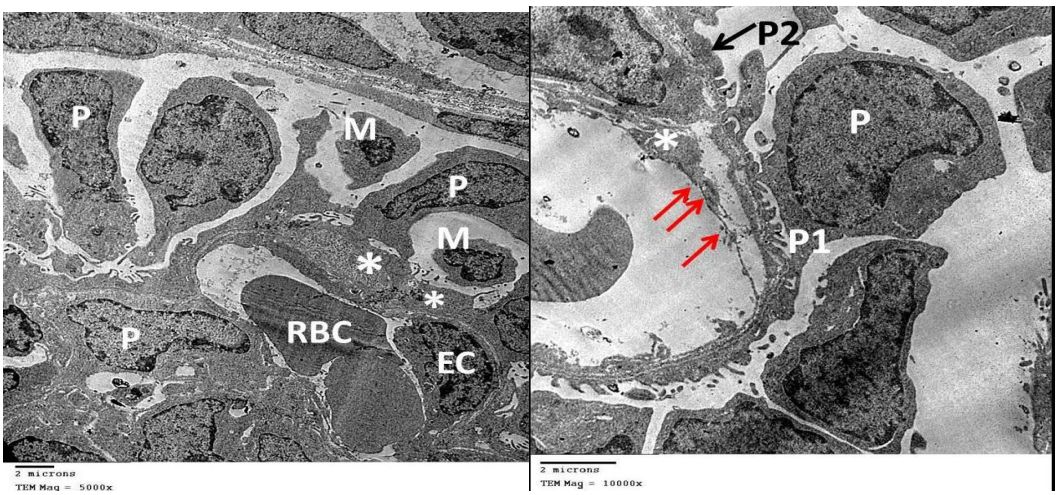

Figure 12: photomicrographs of ultrathin **sections of** the renal corpuscle **of group IIB (PND7) treated albino rat** showing: the renal corpuscle contains dilated blood capillaries which contain the red blood cells (RBC). The glomerular capillary membrane is abnormally thickened (asterisks). The podocyte (P) and mesangial (M) cells are poorly developed. **TEM x 5000.**

Figure 13: photomicrographs of ultrathin **sections of** the renal corpuscle **of group IIB (PND7) treated albino rat** showing: the glomerular filtration membrane has areas of detachment of the endothelial lining (red arrows), areas of abnormal thickening in certain points (asterisk). The podocytes (P) primary processes (P1) appear underdeveloped and the secondary foot processes (P2) are fused at certain points. **TEM x 10000**.

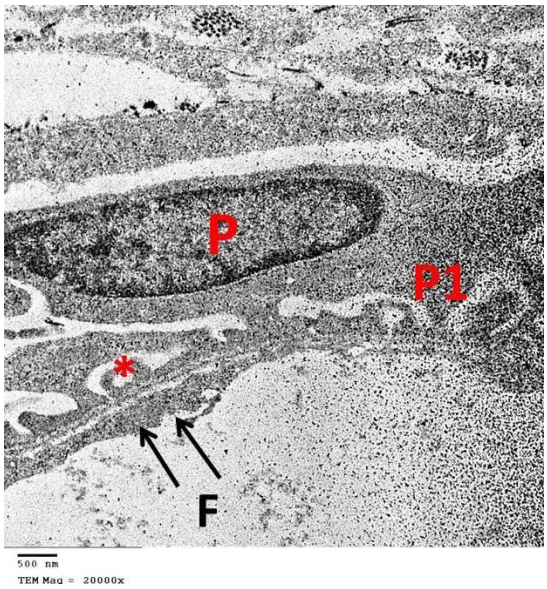

Figure 14: photomicrographs of ultrathin **sections of** the renal cortex **of group IIB (PND7) treated albino rat** showing: the capillary border appears with abnormal thickening along the endothelial lining with decrease in of the endothelial fenestrations (F). The podocytes (P) foot processes (P1) are underdeveloped and secondary processes are fused and hardly seen at certain points (red asterisks). **TEM x 20000.**

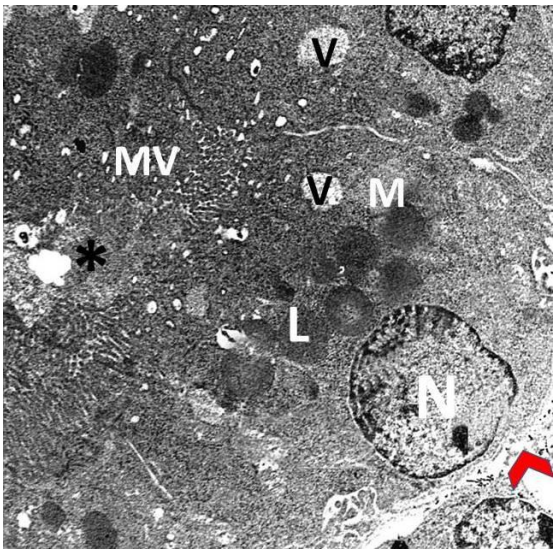

Figure 15: photomicrographs of ultrathin **sections of** the PCT **of group IIB (PND7) treated albino rat** showing: the PCT cell appears with resting on abnormal basement membrane

(arrow head), small nuclei (N), the apical microvilli (MV) appear less dense and disrupted (asterisk), more frequent enlarged cytoplasmic vacuoles (V) with enlarged lysosomes (L). **TEM x 10000.**

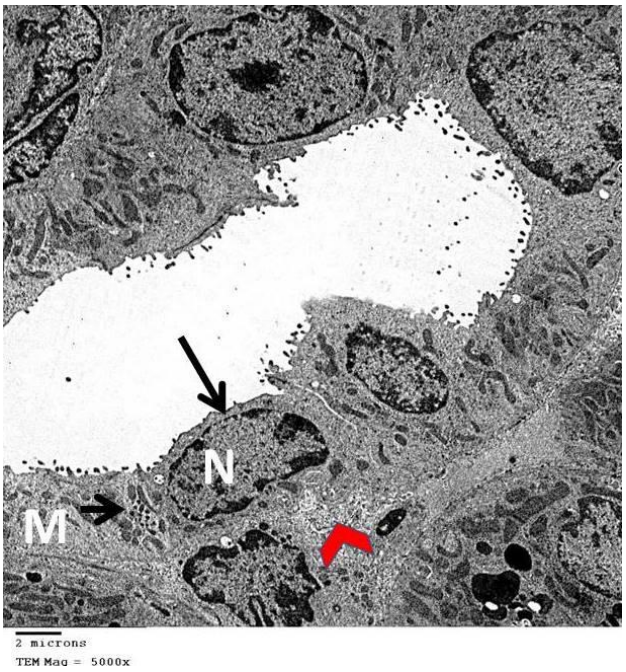

Figure 16 : photomicrographs of ultrathin **sections of** the renal cortex **of group IIB (PND7) treated albino rat** showing some ells of the DCTS are devoid of the apical microvilli (arrow), abnormal basement membrane (arrow head) with oval nuclei (N), fragmented abnormal mitochondria (M). **TEM x 5000.**

DISCUSSION

Kidney damage was irreversible and it might lead to the development of end-stage renal disease. The toxicity of TAM as an anti-estrogen towards multiple organ systems had been reported in a number of contexts and all had been attributed to estrogen receptor independent effects **(Hamad et al., 2015)**. (**Lien et al., 1991)** clarified that the highest levels of TAM and its metabolites were observed in lung, liver, and kidney. In the present study, there were significant decrease in the body weight of both (GD20) IB and IIB (PND7) treated groups. These data are in agreement with the results **(Biegel et al., 1998)** and **(Kuwagata et al., 1999)** who noticed that early neonatal exposure to several synthetic estrogenic agents caused a decrease in body weight in rats and mice. While, (**Clark et al., 1992; Pons and Torres-Aleman, 1993)** explained the reduction of weight under the treatment of TAM might be caused by growth hormone deficiency manifested as growth retardation in the offspring. It is well-documented that estrogenic and anti-estrogenic compounds altered the hypothalamic-pituitary-ovarian feedback and the secretion and regulation of growth hormone are related to

this neuro-endocrine axis**.** Alternatively, (**Heena et al., 2007)** reported that the progressive weight loss observed in the treated animals could be secondary to the progressive renal dysfunction detected in the TAM treated animals.

In the current study, in group II B (PND7) exposed to the oral administration of TAM for 28 days caused nephrotoxicity. The biochemical results showed that significant increase in the nitrogenous end products; serum creatinine, urea and uric acid, which reflect the efficacy of kidney function. This data was in accordance with (**Sofia et al., 2008),** who mentioned that the oral TAM therapy was associated with the disturbances of kidney function tests which was connected with impairment to the vasculature or/and structures of the kidneys**.** Our data was also in accordance with the findings of (**Heena et al., 2007)**. The latter concluded that TAM induced nephrotoxicity through induction of oxidative stress that lead to kidney tissue injury using renal lipid peroxidation as a marker of renal injury. Also, (**Zuhair, 2011)** elucidated the possible mechanism of TAM-induced nephrotoxicity. He reported that nephrotoxicity might be due to the Reactive oxygen species (ROS) that are produced by TAM could damage the glutathione redox system of the kidney and subsequently, induce free radicals production in renal tissue.

The biochemical analysis of this study of (PND7) treated kidney confirmed a highly significant reduction of the serum total proteins and serum albumin. These findings can be supported by (**Weyer et al., 2012)** who reported the finding of tubular dysfunction in itself may cause albuminuria owing to decreased reabsorption of filtered albumin**.** The significant amounts of albumin fragments were excreted in the urine as a result of tubular degradation. In addition, (**Liangos et al., 2006)** added that reduced serum total proteins and serum albumin could be secondary to proteinuria and albuminuria, manifestation of the renal injury. In addition, (**Cunha et al., 1987)** added that the increased incidence of kidney failure was mostly associated with the chemotherapy-induced renal dysfunction. TAM treatment of the pregnant rats induced kidney failure in the neonatal and early postnatal rat pups.

Our data indicated that both (GD20) IB and (PND7) IIB treated groups showed marked histological developmental damage and degeneration when compared with the control group. The tamoxifen treated kidneys developed shrunken atrophied glomeruli with disrupted reduced glomerular tuft of capillaries and dilated capsular space. These findings were in agreement with **(Pandeya et al., 2015)** who reported the histological changes in the kidney of tamoxifen treated animals. The treated kidneys developed extensive degeneration with severe

vasocongestion, edema in the renal parenchyma and wide dilatation of Bowman's capsule. In the current work, in prenatal and postnatal treated groups the PCT and DCT were swollen with loss of some of their nuclei with areas of focal necrosis and some cells of the renal tubules degenerated and had vacuolated cytoplasm with pyknotic and apoptotic nuclei. The previous findings can be explained on the basis of the observations made by (**Saleh et al., 2016)** who concluded that kidneys were target organ for the toxic, pathologic and accumulative effects off TAM in the PCT that induced degeneration and cytoplasmic vacuolation. Moreover, (**Braems et al., 2011)** discussed that maternal exposure to tamoxifen during pregnancy seemed to slow postnatal development in the offspring. During pregnancy, TAM and its metabolites interact with rapidly growing and developing embryonic or fetal tissues. In addition, **(Fadhil and Majeed 2016)** stated that the scientific research on tamoxifen citrate strongly indicated that the kidney was the target organ for the toxicological and pathological effect of tamoxifen citrate, as they tested compound accumulated in the PCT result in degeneration and vacuolation. On the other hand, (**Parlakpinar et al., 2005)** reported that the important mediators of nephrotoxicity with administration of TAM were ROS production and depletion in the cellular thiol system which induced renal damage.

In the present work in both (GD20 AND PND7) treated groups, PAS positive reaction decreased in the brush borders of the PCT and basement membrane of renal tubules and glomerular capillaries. The results could be proved by (**Ganong, 1983)** who explained the decrease in PAS positive materials in most of renal disease, it might be due to decrease in the renal proteins as a result in the increase of the permeability of glomerular capillaries.

In the present study, semithin sections of the PND7 treated kidney albino rat, showed that there were delayed in development of the renal corpuscles. The previous results was in agreement with (**Braems et al., 2011)** who reported that relatively high frequency of severe congenital abnormalities indicates that it is reasonable to stop tamoxifen before pregnancy. They registered 11 babies with higher incidence of congenital malformations, stillbirth and delayed development in the TAM treated pregnant female. Also, (**Cunha et al., 1987)** added that animal and human data suggested that most antineoplastic drugs might have had deleterious effects on the fetus, including increasing incidence of prematurity, intrauterine growth retardation and low birth weight. Also, (**Shaaban, 1975)**; (**Cunha et al., (1987)** and (**Cullins et al., 1994)** reported that tamoxifen can cause harmful effect to the fetus if

administered to pregnant women and therefore should be used cautiously during pregnancy and breast feeding because of the potential for serious adverse reactions in nursing infants.

In the current study, in the electron microscopic examination in group IIB (PND7) revealed that some degenerative changes in the renal corpuscle involved dilated congested capillaries basement membrane, poorly developed podocytes foot processes and decrease in endothelial fenestrations with areas of detachment of the capillary endothelial membrane. In addition, there were abnormalities in the development of the GBM that included thickening and fusion. Most important changes, the Podocytes foot processes were fused to each other's causing abnormal thickening along the parietal layer of the filtration membrane. This detailed description of developmental changes in the TAM treated animals were in accordance with progressive nephropathy alterations in the developing glomerulus. This had been suggested by (**Badawy et al., 2002)** who said that it was attributed to TAM dependent progressive production of ROS. The previous findings were explained by (**Donovan et al., 1994)** who stated that damage to the GBM itself was attributed to ROS attacking the GBM and damaging its matrix structure. While, **(Ricardo et al., 1994 and Aydogan et al., 2008)** added that TAM induced fusion and flattening of foot processes due to direct injury to the podocyte skeleton after exposure to ROS. On the other hand, (**Mohamed and Elsharkawy., 1995)** concluded that the thickened GBM might be developed secondary to compensate increased glomerular permeability and proteinuria**.**

The results were also in accordance with the findings of **(Hinkes et al., 2006); (Macconi et al., 2006)** who confirmed with some pathological situations the architecture of foot processes was lost, a process referred to as effacement. They added that effacement of foot processes can cause glomerular scarring (glomerulosclerosis), leading to impairment of the glomerular filtration and chronic renal failure. Our results are also in accordance with previous reports that indicated Nolvadex (TAM) treatment through an oral route in rats could induce various tissue damage **(Smith et al., 2000)** including brain astrocytes **(Li et al., 1997)**. TAM produced progressive production of ROS and was a major element in the induction of oxidative stress. The latter is a well-documented cause of cells injury and pathogenesis of disease **(Saad and Alrikabi, 2002)**.

In the present work, in group IIB the proximal convoluted tubule, cells appeared with distorted basement membrane and the apical microvilli appeared less dense and disrupted, more frequent enlarged cytoplasmic vacuoles and with enlarged lysosomes. The previous

findings were explained by (**Zahir et al., 1995)** and (**Badawy et al., 2002)** they reported that the administration of Nolvadex caused the production of reactive oxygen species (ROS) or abnormal filtered substances absorbed by tubular epithelial cells, which could damage the cellular elements. In addition, (**Mahmoud and El-Badry, 2001)** added that the oxidative modifications of DNA, protein and lipids by ROS played a role in ageing and disease. These previous data were in accordance with (**Joles et al., 2000)** who mentioned that lysosomes when exposed to toxic insults increase in size and number and undergo phospholipidosis. It has been reported that cytoplasmic accumulation of lysosomes indicates cell injury.

CONCLUSIONS

Tamoxifen induced structural changes in the kidney during pregnancy and breast feeding. Therefore, TAM should not be taken at any time during pregnancy and lactation.

REFERENCES

1. **Aydogan, S.; Yapislar, H.; Artis, S. and Aydogan B (2008):** Impaired erythrocytes deformability in H2O2- induced oxidative stress: Protective effect of L carnosine. Clin Hemorheol Microcirc, 39: 93–98.
2. **Badawy, S.A.; El-Far, F.I. and Amer, H.A. (2002):**Testicular and post testicular role of estrogen in adult male rabbit. Egypt. J. Basic and Appl. Physiol., 1(2): 269-280.
3. **Bancroft, J.D. and Gamble, M. (2013):** Theory and practice of Histological Techniques. The 7th ed. Philadelphia: Churchill Livingstone of Elsevier. PP, 172–186.
4. **Biegel, L.B.; Flaws, J.A. and Hirshfield, A.N.; O'Connor, J.C. et al. (1998):** 90-day feeding and one generation reproduction study in Crj:CD BR rats with 17/3-estradiol. Toxicol. Sci., 10: 116-142.
5. **Braems, B.; Denys, H.; De Wever, O.; Cocquyt, V. and Broecke, R.V. (2011):** Use of Tamoxifen . Before and During Pregnancy. The Oncologist.; 16: 1547–1551.
6. **Butkevich, I.; Khozhai, L.; Mikhailenko, A. and Otellin, V. (2003):** Decreased senotonin level during pregnancy altens monphological and functional chanaetenistics of tonic nociceptiv system in juvenile offspring of the rat. Reprod. Biol.Endocrino13: 1-96.
7. **Clark, J.H., Schrader, W.T. and O'Malley, B.W. (1992):** Mechanisms of action of steroid hormones. In: Textbook of Endocrinology. Philadelphia, Saunders, pp. 35-90.
8. **Colleoni, M.; Gelber, S.; Goldhirsch, A.; Aebi, S. and Castiglione-Gertsch, M. (2006):** Tamoxifen after adjuvant chemotherapy for premenopausal women with lymph

node-positive breast cancer: International Breast Cancer Study Group Trial 13-93. J Clin Oncol, 24: 1332-1341.

9. **Cullins, S. L.; Pridjian, G. and Sutherland, C. M. (1994):** Goldenhar's Syndrome associated with tamoxifen given to the mother during gestation. Lancet, 271: 1905–1906.
10. **Cunha, G.R.; Taguchi, O.; Namikawa, R. et al. (1987):** Teratogenic effects of clomiphene, tamoxifen, and diethylstilbestrol on the developing human female genital tract. Hum Pathol., 18: 1132–1143.
11. **Desai,P.; Nallani,S.; Sane,R.; Moore, L. ;Goodwin, B.; Buckley,D. and Buckley, A. (2002):** Drug Metab.Dispos., 30: 608-612.
12. **Diwan, B. A., Anderson, L. M. and Ward, J. M. (1997):** Proliferative lesions of oviduct and uterus in CD-1 mice exposed prenatally to tamoxifen. Carcinogenesis (Lond.), 18: 2009–2014.
13. **Donovan, K.L.; Davies, M., Coles, G.A. and Williams JD. (1994):** Relative roles of elastase and reactive oxygen species in the degradation of human glomerular basement membrane by intact human neutrophils. Kidney Int., 45: 1555–1561.
14. **Dragan, Y.P.; Fahey, S.; Nuwaysir, E.; Sattler, C.;Babcock, K.; Vaughan,J.; McCague, R. et al.(1996):** The effect of tamoxifen and two of its non-isomerizable fixed-ring analogs on multistage rat hepatocarcinogenesis. Carcinogenesis, 17: 585-94.
15. **Dray,X., Tainturier,M.H., De La Lande, P., Marty,O., Mallet, L., (2000):** Gastroenterol Clin.Biol., 24: 1122-1133.
16. **Elefsiniotis, I.S.; Pantazis, K.D.; Ilias, A.; Pallis, L.; Mariolis, A.; Glynou, I. et al**.; **(2004):** Eur.J.Gastroenterol. Hepatol., 16: 593-598.
17. **Fadhil, S. R. and Majeed, S. K. (2016):** Histo Toxic and Pathologicl Study of Tamoxifen Citrate on The Kidney of Female Rats. Journal of Agriculture and Veterinary Science, 9: 70-74.
18. **Fisher, B.; Costantino, J.P.; Wickerham, D.L.; Cecchini, R.S.; Cronin, W.M. et al. (2005):** Tamoxifen for the prevention of breast cancer: current status of the National Surgical Adjuvant Breast and Bowel Project P-1 study. J Natl Cancer Inst., 97: 1652-1662.
19. **Ganong, W.F. (1983):** ''Review of medical physiology''. 11th ed.Lang Medical publication, Los Anglos, California. pp. 459-463.
20. **Glauert A.M. and Lewis P.R. (1998):** Biological specimen preparation for transmission electron microscopy. 1st ed. Princeton University Press. London. pp 135-44.

21. **Hamad, R.; Calpurnia, J.; Punithavathi, R.; Riyaz, M. et al. (2015):** Honey feeding protects kidney against cisplatin nephrotoxicity through suppression of inflammation. Clinical and Experimental Pharmacology and Physiology, 42: 843-848.
22. **Heena, T.; Parvez, S.; Rehman, H.; Dev-Banerjee,B.; Siemen, D. and Raisuddin,S. (2007):** Nephrotoxicity and its prevention by taurine in tamoxifen induced oxidative stress in mice. Human & experimental toxicology, 26: 509-518.
23. **Hinkes, B.; Wiggins, R.; Gbadegesin, R. et al. (2006):** Positional cloning uncovers mutations in PLCE1 responsible for a nephrotic syndrome variant that may be reversible. Nat Genet., 38: 1397–1405.
24. **Jin, Y.; Desta, Z.; Stearns, V.; Ward, V.; Skaar,T. and Storniolo, A. M. (2005):** J.Nat.Cancer Inst., 97: 30-39.
25. **Joles, J.A.; Kunter, U.; Janssen, U.; Kriz, W.; Rabelink, T.J. et al. (2000):** Early mechanisms of renal injury in hypercholesterolemic or hypertriglyceridemic rats. J Am Soc Nephrol., 11: 669–683.
26. **Kintzel, P. E. and Robert, T. D. (1995):** Anticancer drug renal toxicity and elimination: dosing guidelines for altered renal function. Cancer treatment reviews, 21: 33-64.
27. **Kuwagata, M. ; Saito Y.; Yoshimura, S. and Nagao,T. (1999):** Reproductive Effects of Early Neonatal Exposure to Diethylstilbestrol or Tamoxifen in Rats. Cong. Anom., **39:** 295-307.
28. **Lazzeroni, M.; Serrano, D.; Dunn, B. K.; Heckman, B. M. and Decensi, A. (2012):** Oral low dose and topical tamoxifen for breast cancer prevention: modern approaches for an old drug Breast Cancer Research, 14: 214-220.
29. **Li, D.; Yvonne, D.; Craig, J.; Mianying, W.; and Henry, C. P. (1997):** Effects of chronic administration of tamoxifen and toremifene on DNA adducts in rat liver, kidney, and uterus. Cancer research, 57: 1438-41.
30. **Liangos, O.; Ron, W.; John, W.; Lorilyn, P.; Brian, J. P. and Bertrand, L. J. (2006):** Epidemiology and outcomes of acute renal failure in hospitalized patients: a national survey. Clinical Journal of the American Society of Nephrology, 1: 43-51.
31. **Lien, E. A.; Einar, S. and Per, M. (1991):** Ueland. Distribution of tamoxifen and its metabolites in rat and human tissues during steady-state treatment. Cancer research, 51: 4837-44.
32. **Lo, S.S. and Vogel, V.G. (2004):** Endocrin prevention of breast cancer using selective oestrogen receptor modulators (SORMS). Best. Pract. Res. Clin. Endocrinol. Metab., 18: 97-111.

33. **Macconi, D.; Bonomelli, M.; Benigni, A.; Plati, T., Sangalli, F.; Longaretti, L. et al. (2006):** Pathophysiologic implications of reduced podocyte number in a rat model model of progressive glomerular injury. Am J Pathol., 168: 42–54.
34. **Mahmoud, F.Y. and El-Badry, M. (2001):** Histological effects of gentamicin intake during pregnancy on the liver and kidney of the fetus and mother of albino rat. Egypt J Anat, 24: 35–57.
35. **Mohamed, S.A. and Elsharkawy, S.A. (1995):** Histological study of early and late nephrotoxicity and endothelial cytotoxicity of ionic and non-ionic contrast media. Egypt J Anat, 18: 115–132.
36. **Paget, G.E. and Barnes, J.M. (1964):** Evalution of Drug Activites and pharmacokinetics. Acadenic Press, 1: 135-136.
37. **Pandeya, S. K.; Ghosh, S. ; Maiti, P.; M. and Haldar, C. (2014):** Therapeutic efficacy and toxicity of tamoxifen loaded PLA nanoparticles for breast cancer. International Journal of Biological Macromolecules, 72: 309–319.
38. **Parlakpinar, H.; Tasdemir, S.; Polat, A.; Bay-Karabulut, A. N; Ucar, M. A. (2005):** Protective role of caffeic acid phenethyl ester (cape) on gentamicin-induced acute renal toxicity in rats. Toxicology, 207: 169–177.
39. **Parvez, S.; Tabassum, H.; Rehmana, H.; Dev-Banerjee, B. et al. (2006):** Toxicology, 225: 109-118.
40. **Pons, S. and Torres-Aleman, I. (1993):** Estradiol modulates insulin-like growth factor I receptors and binding proteins in neurons from the hypothalamus. Neuroendocinol., 5: 267-271.
41. **Ricardo, S.D.; Bertram, J.F. and Ryan, G.B. (1994):** Reactive oxygen species in puromycin aminonucleoside nephrosis: in vitro studies. Kidney Int., 45: 1057–1069.
42. **Rosner B. (1990):** Fundamental of biostatistics. PWS-Kent Publishing Co.: Boston. pp.18-23.
43. **Saad, S.Y. and Al-Rikabi, A.C. (2002):** Protection effects of taurine supplementation against cisplatin-induced nephrotoxicity in rats. *Chemotherapy*, **48**: 42–48.
44. **Saleh, H.; Mohamed, B. and Marie, M. S. (2016):** Sodium Butyrate Attenuates Nephrotoxicity Induced by Tamoxifen in Rats. Journal of Applied Pharmaceutical Science, 6: 066-072.
45. **Sato, T.; Ohta, Y.; Okamura, H.; Hayashi, S. and Iguchi, T. (1996):** Estrogen receptor (ER) and its messenger ribonucleic acid expression in the genital tract of female mice exposed neonatally to tamoxifen and diethylstilbestrol.Anat. Rec., 244: 374–385.

46. **Shaaban, M.M. (1975):** Suppression of lactation by an antiestrogen, tamoxifen. Eur J Obstet Gynecol Reprod Biol., 4: 167-9.
47. **Smith, L.L.; Brown, K.; Crathew, p. et al. (2000):** Chemoprevention of breast cancer by tamoxifen: risks and opportunities. Crit. Rev. Toxicol., 30(5): 571-594.
48. **Sofia, A.B.; Culleton, B. F.; Marcello, Tonelli, S. W.; Jennifer, K. M. et al. (2008):** Oral estrogen therapy in postmenopausal women is associated with loss of kidney function. Kidney international, 74: 370-76.
49. **Tan-Chiu, E.; Wang, J.; Castantino, J.P. et al. (2003):** Effect of tamoxifen on benigen breast disease in woman at high risk for breast cancer. J. Natl. Cancer Inst, 19: 95(4): 302-307.
50. **Weyer, K. Nielsen, R. , Christensen, E. , and Birn, H. (2012):** Generation of Urinary Albumin Fragments Does Not Require Proximal Tubular Uptake. J Am Soc Nephrol, Apr; 23(4): 591–596.
51. **Zahir, F.I.; Elzahwy, A.K.; Ismail, Z.M.K. and Mohamed, S.A. (1995):** Effects of ketamine and diazepam on the morphology of the kidney of rabbit: an electron microscopic study. Assiut Vet Med J, 34: 1–12.
52. **Zuhair, Z. (2011):** The role of vitamin C in alteration of enzymes responsible of energy metabolism induced by administration of tamoxifen to mouse. Advances in Biological Chemistry, 1: 15.